

Improving joint features and tensile shear properties of friction stir lap welded joint by an optimized bottom-half-threaded pin tool

Y. M. Yue¹ · Z. L. Zhou¹ · S. D. Ji¹ · L. G. Zhang¹ · Z. W. Li²

Received: 19 May 2016 / Accepted: 10 October 2016 / Published online: 19 October 2016
© Springer-Verlag London 2016

Abstract To increase the lap shear failure load of friction stir lap welding (FSLW) joint, a tool with a bottom-half-threaded pin was designed in the present study. Using 7N01-T4 aluminum alloy as the research object, tools with the bottom-half-threaded pin and the traditional full-threaded pin were used to fabricate lap joints. Results showed that the thread end position on the pin greatly influenced the material flow behavior. The material concentrated zone using the bottom-half-threaded pin mainly located above the lap interface, which is beneficial to suppress the hook and cold lap. The lap shear failure load of the FSLW joint using the bottom-half-threaded pin was 17,644.7 N, which is equal to 122.8 % of the joint using the full-threaded pin.

Keywords Friction stir lap welding · Bottom-half-threaded pin · Hook · Cold lap · Lap shear failure load

1 Introduction

Friction stir welding (FSW) is a solid-state joining method which was invented by The Welding Institute

(TWI) in 1991 [1]. With low power requirement, small distortion and so on, FSW joints have been used in aerospace, automobile and ship building in the recent years [1]. 2xxx and 7xxx series aluminum alloys can be successfully weld by FSW instead of traditional fusion welding [2, 3]. Defects such as porosity, hot crack, and element loss, which always appear in the fusion welding joint, can be avoided by FSW [4]. Beside butt welding joint, friction stir lap welding (FSLW) joint is another common FSW joint feature. Lap joints are extensively used in the transportation industries, such as aircraft skins and ship decks [5].

As the typical features of the lap joints, hook and cold lap are the key factors affecting the joint lap shear properties. Some papers about influence of the welding parameters on the hook and cold lap morphologies have been reported [6, 7]. Shirazi et al. [6] found out that hook height decreased with increasing the welding speed. Fadaeifard et al. [7] reported that heights of both hook and cold lap decreased with increasing the rotational speed. In fact, besides the welding parameters, tool geometry has an important influence on size, shape, and location of hook and cold lap [8]. Using three different tools (a cylindrical tool and two conical tools with different taper angles), Costa et al. [9] concluded that the conical tool with smaller taper angle fabricated lap joints with better mechanical properties. Yang et al. [10] found out that the triangular pin improved the lap shear failure load of FSLW joint by suppressing the hook and cold lap.

Material flow behavior is one of the key factors affecting joint mechanical properties. The thread on pin can accelerate material flow during welding [11]. However, compared with butt welded joints, few papers focused on the pin thread in FSLW. Using four different

✉ S. D. Ji
superjsd@163.com

✉ Z. W. Li
qingdaolzw@163.com

¹ Faculty of Aerospace Engineering, Shenyang Aerospace University, Shenyang 110136, People's Republic of China

² State Key Laboratory of Advanced Welding and Joining, Harbin Institute of Technology, Harbin 150001, People's Republic of China

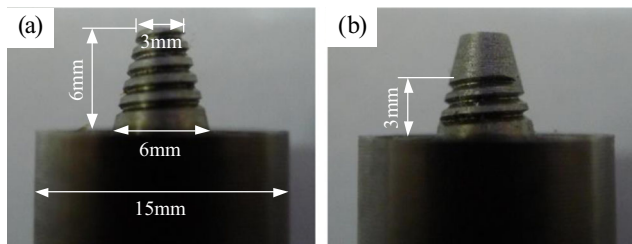


Fig. 1 Tools used in experiment. **a** Full-threaded pin. **b** Bottom-half-threaded pin

pins (a conical thread pin, a cylindrical conical thread pin, a stepped conical thread pin, and flared tri-flute pin tool), Casalino et al. [4] found out that the stepped conical thread pin fabricated joint with the lowest hook and highest lap shear failure load. Mohammadi et al. [12] found out that the threaded pin owned better performance than the smooth pin when welding dissimilar AZ31B Mg and 6061 Al alloys. Moreover, the reverse-threaded pin designed by Yue et al. [13] fabricated joint with bigger effective sheet thickness (EST), bigger effective lap width (ELW), and better lap shear properties. In the present study, a tool with a bottom-half-threaded pin was designed and manufactured, aiming at suppressing the hook and cold lap for the purpose of improving the tensile shear failure load of FSLW joint.

2 Experimental

Alclad 7N01-T4 aluminum alloy with 4 mm thickness was chosen as the base material (BM). Surfaces of all the plates were cleaned by sandpapers before welding. The FSW-3LM-4012 machine was used during the experiment. Detailed dimensions of the two tools used in the present study are shown in Fig. 1. Different from the tool in Ref. [14], thread on pin starts from the pin bottom and ends at the pin middle region (Fig. 1b), which is called bottom-half-threaded pin. All the joints were welded according to configuration A, meaning the advancing side of the joint bears the main load during

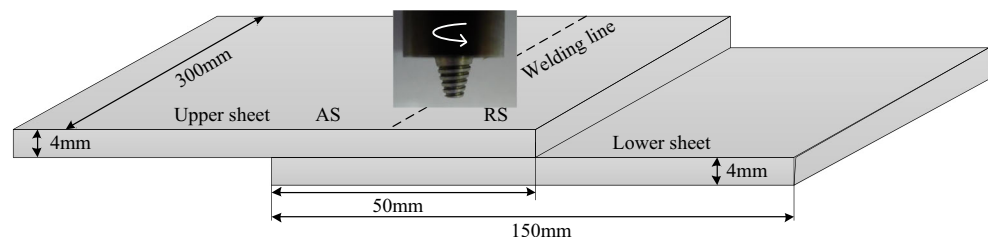
the lap shear test (Fig.2) [15]. The rotational speed was 1000 rpm. The welding speed was 50 mm/min. Shoulder plunge depth was 0.2 mm. Tilt angle during welding was 2.5°. After welding, electrical discharge cutting machine was used to cut metallographic and lap shear specimen. Width of the lap shear specimen was 40 mm. Metallographic specimen was polished by sandpaper and etched with Keller's reagent (2 ml hydrofluoric acid, 3 ml hydrochloric acid, 5 ml nitric acid, and 190 ml water). Metallographic analysis was performed on optical microscopy (OM, OLYMPUS-GX71). Lap shear specimens were tested on computer-controlled universal tensile testing machine (INSTRON-8801). After that, fracture positions were observed on a stereoscopic microscope (ZSA403) and fracture surfaces were analyzed using a scanning electron microscope (SEM, SU3500).

3 Results and discussion

3.1 Cross section of the lap joints

Figure 3 shows the cross sections of the joints using the two different tools. It can be seen that the two cross sections show rather different morphologies. As shown in Fig. 3a, hook shows an upward bending morphology at the advancing side (AS). At the retreating side (RS), cold lap firstly shows an upward bending morphology and then bends downwards into the stir zone (SZ). Material flow behavior during welding can be divided into pin-driven material flow and shoulder-driven material flow. At the AS, hook morphology is mainly affected by the pin-driven material flow. In the present study, plastic material flow downwards along the pin thread. After released from the thread, plastic material gradually accumulates, forming a concentrated zone. As the welding process goes on, the concentrated zone gradually becomes bigger and forces the material of the thermal-mechanically affected zone (TMAZ) to flow upwards. Together with the TMAZ, both hook and cold

Fig. 2 Schematic diagram of the FSLW process



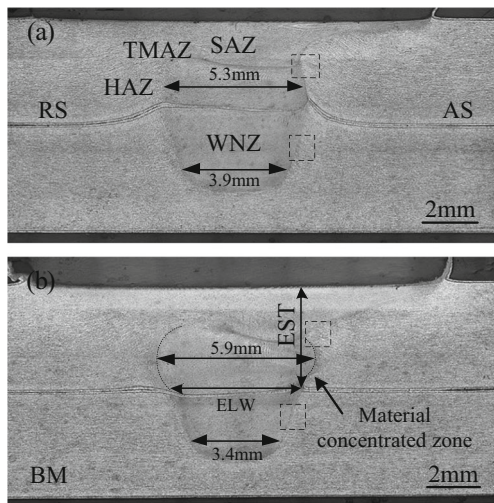


Fig. 3 Cross sections of the lap joints using the full-threaded pin (a) and the bottom-half-threaded pin (b)

lap firstly show upward bending morphologies, as shown in Fig. 3a. Besides, plastic material flows from AS to RS as the rotation of the tool. After combined with the pin-driven material, plastic material flows into the cavity left by the forward movement of the pin. Hence, the cold lap shows a downward bending morphology in the SZ.

Compared with the traditional full-threaded pin, the bottom-half-threaded pin has no thread on its pin tip region. Lin et al. [16] and Fujimoto et al. [17] stated that the pin thread can accelerate the material flow. Ji et al. [11] reported that the threaded pin caused more material accumulating near the pin tip. As shown in Fig. 3a, there is a material concentrated zone near pin tip region. The width of the SZ bottom is 3.9 mm. By contrast, much less material accumulates at the pin tip region using the bottom-half-threaded pin (3.4 mm), resulting in much smaller pressure on the TMAZ of lower sheet. Hence, hook and cold lap using the bottom-half-threaded pin are much smaller than those using the full-threaded pin. As shown in Fig. 1b, thread of the bottom-half-threaded pin ends near the lap interface. After released from the thread, lots of the plastic material concentrates above the lap interface. Therefore, an obvious material concentrated zone can be seen above the lap interface, as shown in Fig. 3b. Width of the SZ above the lap interface using the bottom-half-threaded pin is 5.9 mm, which is much bigger than that using the full-threaded pin (5.3 mm). For lap joint, effective sheet thickness (EST) and effective lap width (ELW) are two most common variables that are used to describe hook and cold lap morphologies. EST refers to the minimum distance from hook tip or cold lap

Fig. 4 Microstructure of joints. a BM. b SAZ. c WNZ

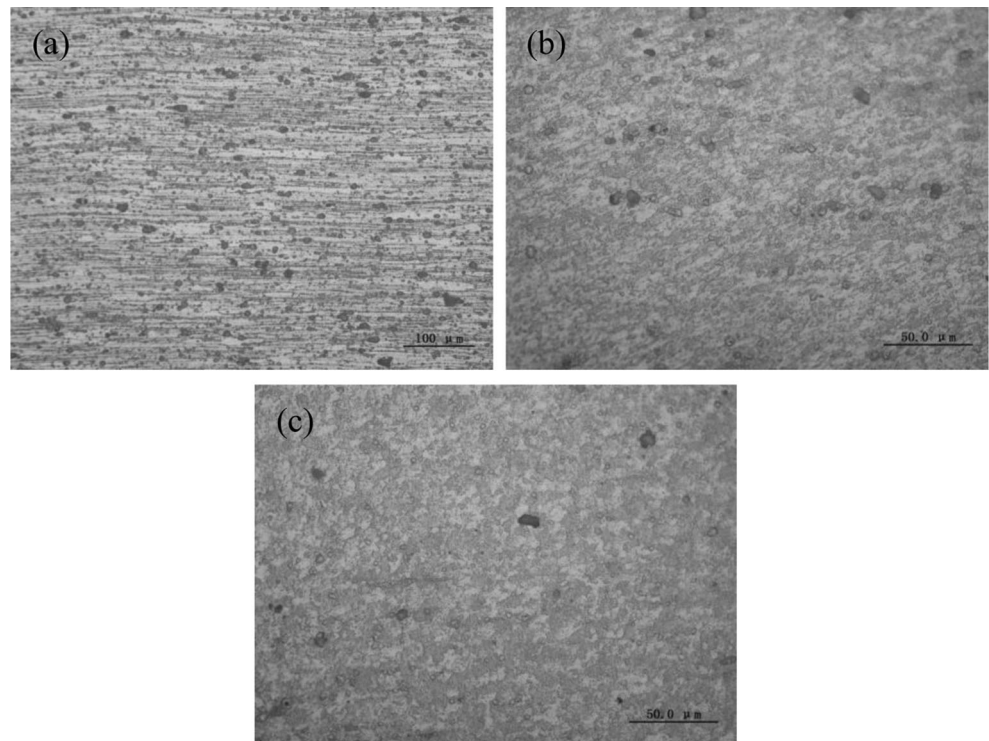
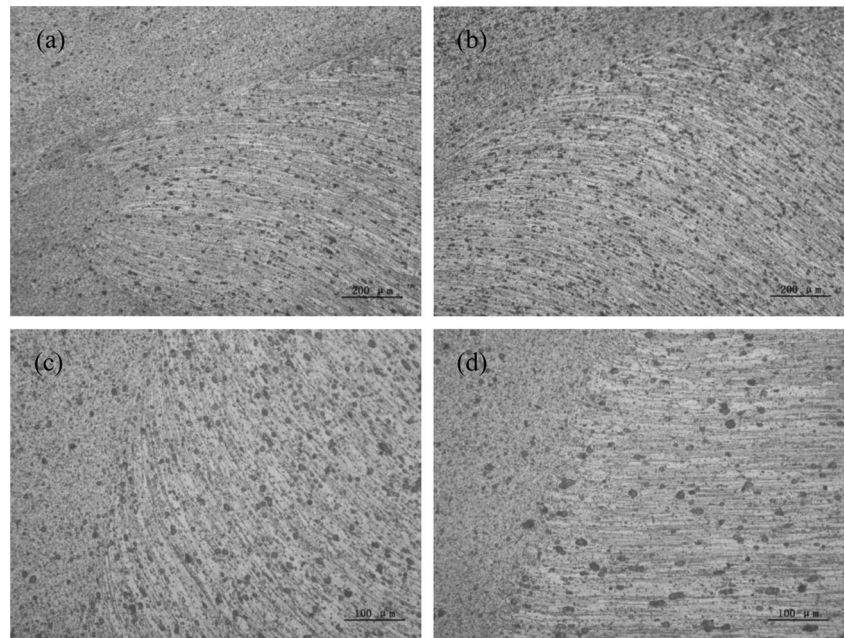


Fig. 5 Microstructure of the TMAZs. **a** TMAZ of the upper sheet using the full-threaded pin. **b** TMAZ of the upper sheet using the bottom-half-threaded pin. **c** TMAZ of the lower sheet using the full-threaded pin. **d** TMAZ of the lower sheet using the bottom-half-threaded pin



highest point to joint upper surface. ELW refers to the bonding width from AS to RS. Configuration A joint was mainly used in this study; hence, the EST above the hook is taken into consideration. As shown in Fig. 3, EST and ELW values using the full-threaded pin are 2.8 and 5.3 mm. For bottom-half-threaded pin, the EST and ELW of joint are respectively 3.7 and 5.0 mm.

Similarly, tensile shear properties of the friction stir spot welding (FSSW) joint are significantly affected by hook [18]. Li et al. [19] effectively eliminated the hook and improved mechanical properties of the FSSW joint using a pinless tool. Based on the hook formation mechanism, the pinless tool reported by Li et al. [19] can also be used to suppress or even eliminate hook of lap joint. However, the pinless tool is more suitable to

weld thin sheets. When the upper sheet is thick, bottom-half-threaded pin in this study is a better choice from the viewpoints of suppressing the hook and cold lap.

3.2 Microstructure of the lap joints

As marked in Fig. 3a, cross section can be divided into SZ, TMAZ, heat-affected zone (HAZ), and BM. SZ can be further divided into shoulder-affected zone (SAZ) and welding nugget zone (WNZ). Figure 4 shows the microstructure of FSLW joint at different regions. BM is characterized with elongated lath-shaped grains, as shown in Fig. 4a. During welding, both WNZ and SAZ are subjected to intense mechanical stirring by rotational tool. Undergone temperature

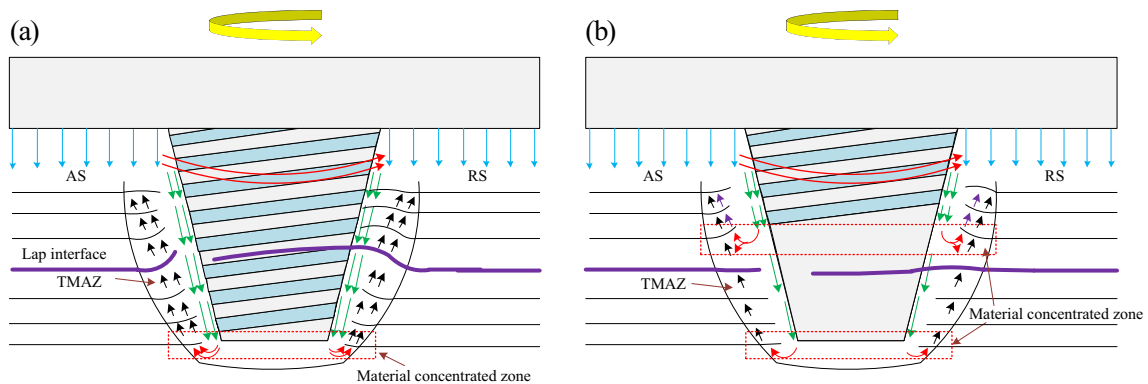


Fig. 6 Material flow behavior during welding. **a** Full-threaded pin. **b** Bottom-half-threaded pin

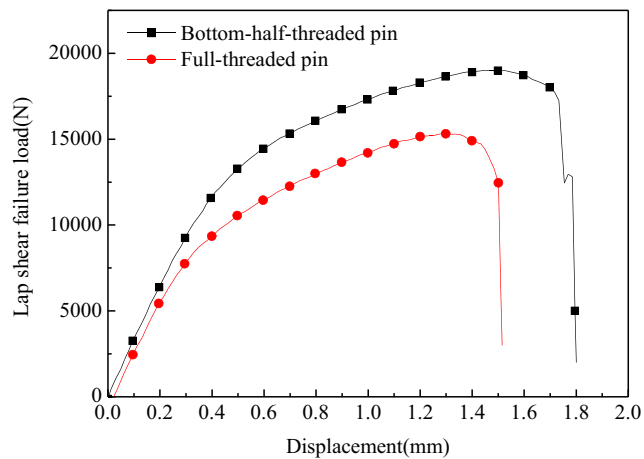


Fig. 7 Load-displacement curves of FSLW joints by different two pins

higher than the recrystallization temperature, SAZ and WNZ are both composed of fine and equiaxed grains (Fig. 4b, c).

TMAZ material is heated and stirred by the tool, resulting in deformed and bending grains (Fig. 5a–d). However, undergone different material flow behaviors, the TMAZ morphologies at different regions are different [20–22]. Figure 5a, b shows the TMAZ material of the upper sheet using the two different tools. It can be seen that the upward bending trend of the TMAZ using the bottom-half-threaded pin is much bigger than that using the full-threaded pin. For full-threaded pin, the material concentrated zone mainly locates at the lower sheet, as shown in Fig. 3a. Undergone long transfer distance, the upward pushing force is largely weakened. Combined with the big forging force exerted by the shoulder, TMAZ material then presents a downward flow trend as the cold lap, as shown in Fig. 5a. As shown in Fig. 3b, the material concentrated zone mainly locates above the lap interface, much less transfer distance results into much bigger upward pushing force. Therefore, the upward flow trend of the TMAZ using the bottom-half-threaded pin is severer. Figure 5c, d show the TMAZs of the lower sheet using the two different pins. Different from the TMAZs of the upper

sheets, the upward flow trend using the full-threaded pin is severer than that using the bottom-half-threaded pin. As previously discussed, much less material concentrates at the pin tip region using the bottom-half-threaded pin. Hence, rather flat flow trend can be observed in Fig. 5d. From the abovementioned analysis, the material flow behavior using the two different pins can be concluded in Fig. 6, which decides the joint cross-section morphologies.

3.3 Lap shear failure load and fracture modes

Figure 8 shows the load-displacement curves using the two different pins. After reaching the highest load point, both the two curves firstly descend slowly and then quickly. The displacement by the bottom-half-threaded pin is bigger than that by the full-threaded pin. The average failure load of the joints by full-threaded pin is 14,372.0 N, while the average failure load by the bottom-half-threaded pin reaches 17,644.7 N. Our previous study proved that lap shear failure load of the joint is determined by both the fracture modes and then the EST or ELW values (Fig. 7) [23]. In this study, only shear fracture mode was attained, as shown in Fig. 8. Hence, the ELW and its metallurgic bonding effect play a more important role on joint lap shear properties. Although the ELW value using the bottom-half-threaded tool is a little smaller, the big pressure induced by the material concentrated zone greatly increases the metallurgical bonding effect of the cold lap. Hence, the lap shear properties of the joint using the bottom-half-threaded pin are bigger. Similar to cold lap, crack also appears in hook. For configuration A, crack has two possible propagation paths. One is along TMAZ/WNZ interface and through SAZ to upper sheet surface. The other is along cold lap and through the WNZ. Hence, small cracks can be observed at the TMAZ/SZ interface on both joints (Fig. 8).

Figure 9 shows the typical fracture morphologies of the joints. Different regions were taken from the regions A, B, C, and D marked in Fig. 8. It is seen that all the

Fig. 8 Fracture positions of the lap joints by different pins. **a** Full-threaded pin. **b** Bottom-half-threaded pin

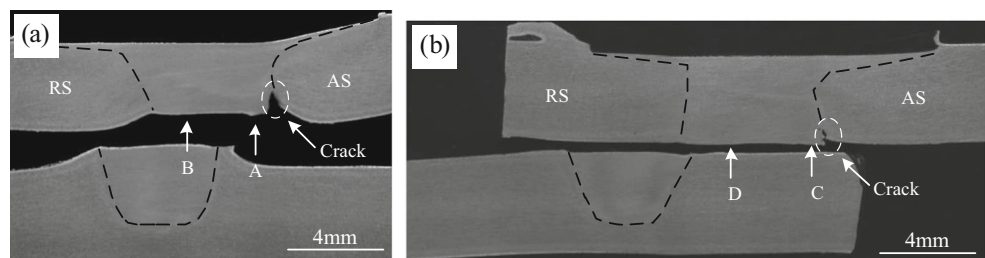
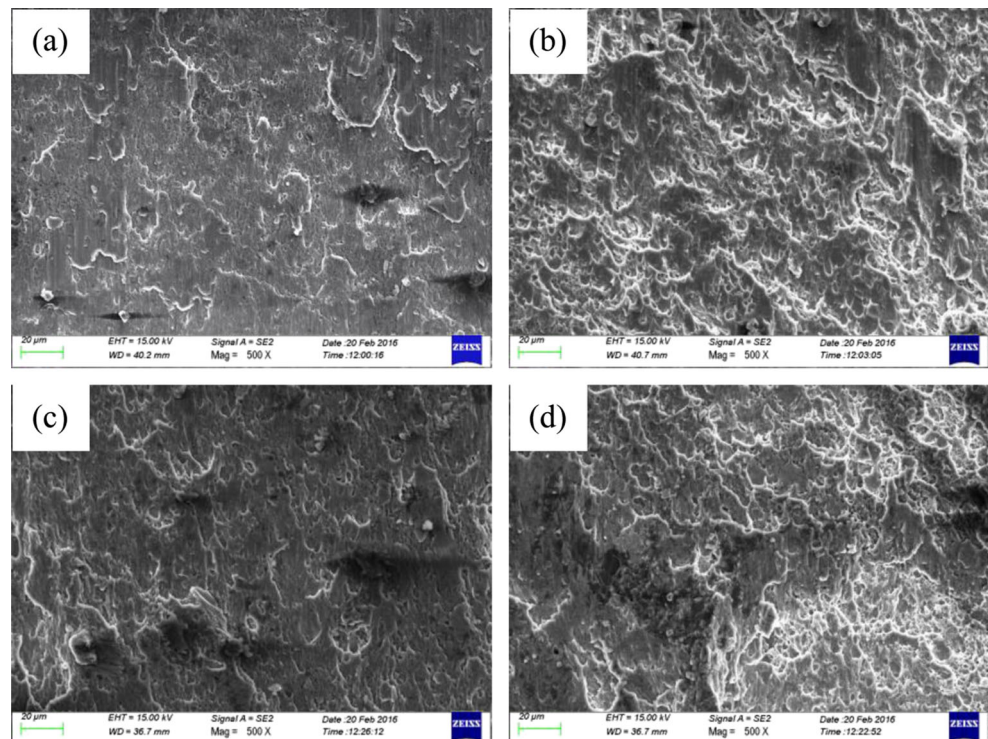


Fig. 9 Fracture morphologies of lap joints. **a** Region A marked in Fig. 8a. **b** Region B in Fig. 8a. **c** Region C in Fig. 8b. **d** Region D in Fig. 8b



fracture surfaces present plenty of dimples with different sizes, indicating the ductile fracture. Figure 9a, c shows the regions near the hook region. Therefore, a small quantity of shallow dimples can be observed. Figure 9b, d shows the middle regions of the cold lap. Hence, numbers and depths of the dimples are increased compared with the hook regions.

4 Conclusions

A new tool with a bottom-half-threaded pin was successfully designed to improve joint feature and the lap shear failure properties of FSLW joint. Microstructure and mechanical properties of the joints using the two tools were studied and compared. Based on the investigation, the following conclusions can be drawn:

1. Thread end position largely changes the material flow behavior during welding. When using the bottom-half-threaded pin, the material concentrated zone mainly locates above the lap interface, which is beneficial to suppress the hook and cold lap.
2. Lap shear failure load of FSLW joint by the bottom-half-threaded pin reaches 17,644.7 N, up to 122.77 % of joint

by full-threaded pin. Shear failure mode is attained by the different two pins.

Acknowledgments This work is supported by the National Natural Science Foundation of China (No. 51204111), the Natural Science Foundation of Liaoning Province (No. 2014024008).

References

1. Chen YH, Quan NI (2012) Interface characteristic of friction stir welding lap joints of Ti/Al dissimilar alloys. *Trans Nonferrous Met Soc China* 22(2):299–304
2. Cantin GMD, David SA, Thomas WM, Lara-Curzio E, Babu SS (2005) Friction skew-stir welding of lap joints in 5083-O aluminum. *Sci Technol Weld Join* 10(3):268–280
3. Song YB, Yang XQ, Cui L, Hou XP, Shen ZK, Xu Y (2014) Defect features and mechanical properties of friction stir lap welded dissimilar AA2024-AA7075 aluminum alloy sheets. *Mater Des* 55:9–18
4. Zhang ZH, Li WY, Shen JJ, Chao YJ, Li JL, Ma YE (2013) Effect of backplate diffusivity on microstructure and mechanical properties of friction stir welded joints. *Mater Des* 50:551–557
5. Wan L, Huang YX, Lv ZL, Lv SX, Feng JC (2014) Effect of self-support friction stir welding on microstructure and microhardness of 6082-T6 aluminum. *Mater Des* 55:197–203
6. Salari E, Jahazi M, Khodabandeh A, Nanesa HG (2014) Influence of tool geometry and rotational speed on mechanical properties and defect formation in friction stir lap welded 5456 aluminum alloy sheets. *Mater Des* 58:381–389

7. Shirazi H, Kheirandish S, Safarkhanian MA (2015) Effect of process parameters on the macrostructure and defect formation in friction stir lap welding of AA5456 aluminum alloy. *Measurement* 76: 62–69
8. Fadaeifard F, Matori KA, Toozandehjani M, Daud AR, Ariffin MKAM, Othman NK, Gharavi F, Ramzani AH, Ostovan F (2014) Influence of rotational speed on mechanical properties of friction stir lap welded 6061-T6 Al alloy. *Trans Nonferrous Met Soc China* 24(4):1004–1011
9. Cederqvist L, Reynolds AP (2001) Factors affecting the properties of friction stir welded aluminum lap joints. *Welding* 80(12):281–287
10. Costa MI, Verdera D, Costa JD, Leitao C, Rodrigues DM (2015) Influence of pin geometry and process parameters on friction stir lap welding of AA5754-H22 thin sheets. *J Mater Process Technol* 225:385–392
11. Yang Q, Li X, Chen K, Shi YJ (2011) Effect of tool geometry and process condition on the strength of a magnesium friction stir lap linear weld. *Mater Sci Eng A* 528(6):2463–2478
12. Ji SD, Shi QY, Zhang LG, Zou AL, Gao SS, Zan LV (2012) Numerical simulation of material flow behavior of friction stir welding influenced by rotational tool geometry. *Comput Mater Sci* 63:218–226
13. Mohammadi J, Beh namian Y, Mostafaei A, Gerlich AP (2015) Tool geometry, rotation and travel speeds effects on the properties of dissimilar magnesium/aluminum friction stir welded lap joints. *Mater Des* 75:95–112
14. Yue Y, Li Z, Ji S, Huang Y, Zhou Z (2016) Effect of reverse-threaded pin on mechanical properties of friction stir lap welded alclad 2024 aluminum alloy. *J Mater Sci Technol* 32(7):671–675
15. Li Z, Yue Y, Ji S, Chai P, Wang L (2016) Optimal design of thread geometry and its performance in friction stir spot welding. *Mater Des* 94:368–376
16. Li Z, Yue Y, Ji S, Chai P, Zhou Z (2016) Joint features and mechanical properties of friction stir lap welded alclad 2024 aluminum alloy assisted by external stationary shoulder. *Mater Des* 90:238–247
17. Lin YC, Chen JN (2015) Influence of process parameters on friction stir spot welded aluminum joints by various threaded tools. *J Mater Process Technol* 225:347–356
18. Fujimoto M, Koga S, Abe N, Sato SY, Kokawa H (2009) Analysis of plastic flow of the Al alloy joint produced by friction stir spot welding. *Weld Int* 23(8):589–596
19. Yin YH, Sun N, North TH, Hu SS (2010) Hook formation and mechanical properties in AZ31 friction stir spot welds. *J Mater Process Technol* 210:2062–2070
20. Li WY, Li JF, Zhang ZH, Gao DL, Wang WB, Dong CL (2014) Improving mechanical properties of pinless friction stir spot welded joints by eliminating hook defect. *Mater Des* 62:247–254
21. Chowdhury SM, Chen DL, Bhole SD, Cao X (2010) Tensile properties of a friction stir welded magnesium alloy: effect of pin tool thread orientation and weld pitch. *Mater Sci Eng A* 527(21):6064–6075
22. Cao X, Jahazi M (2011) Effect of tool rotational speed and probe length on lap joint quality of a friction stir welded magnesium alloy. *Mater Des* 32(1):1–11
23. Liu HJ, Zhao YQ, Hu YY, Chen SX, Lin Z (2015) Microstructural characteristics and mechanical properties of friction stir lap welding joint of alclad 7B04-T74 aluminum alloy. *Int J Adv Manuf Technol* 78:1415–1425